Performance of Packed Columns:

IX. Simulation of a Packed Column

H. L. SHULMAN, W. G. MELLISH, and W. H. LYMAN

Clarkson College of Technology, Potsdam, New York

A model is described which may be used to simulate a packed column for countercurrent gas-phase controlled absorption with liquid-phase reaction. The model consists of a number of continuous stirred-tank reactors in parallel with equal volumes and mass transfer areas. A distribution is presented which uses one parameter to determine the fraction of total liquid throughput going to each reactor. The model successfully predicts all responses, including those of $K_g a$ versus time for no reaction, $K_g a$ versus inlet acid normality, and $K_g a$ versus inlet gas concentration for liquid-phase reaction for the systems ammonia-water and ammonia-sulfuric acid. It also explains the increase in mass transfer obtained by pulsing and controlled cycling.

A simple model was proposed previously (*14*) to explain the large observed differences between the gas-phase mass transfer coefficients for vaporization and absorption. The model was composed of stagnant liquid pockets with holdup h_s and liquid which flows rapidly over the packing corresponding to the operating holdup h_o. The sum of the two holdups is h_t, the total holdup. It was then assumed that vaporization can take place from the total surface area which is proportional to h_t and that absorption can take place only on the rapidly moving surface area which is proportional to h_o, because the stagnant pockets become saturated and ineffective. The correlation

$$\frac{k_g a_{\text{vap}}}{k_g a_{\text{abs}}} = \frac{a_{\text{vap}}}{a_{\text{abs}}} = \frac{h_t}{h_o} \tag{1}$$

was obtained and shown to represent the data. However, there are no completely stagnant pockets in a packed column, and previous dye dispersion (*16*) and particle velocity (*13*) studies in this series showed that the pockets have widely varying residence times from fractions of a second up to 5 to 10 min. The residence times of many pockets were found to be functions of time, probably due to the complex flow geometry above the pockets investigated. The flow was found to be laminar over the outside surfaces of rings, laminar or turbulent in pockets, and turbulent at ring junctions. Thus a wide range of conditions was found from slow moving laminar flow to rapid and complete mixing and even periodic renewal every few seconds by splashing.

Most workers in the field of absorption accompanied by chemical reaction have considered only the liquid-phase mass transfer coefficient and neglected the gas-phase coefficient, particularly for systems where absorption with no reaction is liquid-phase controlled. These systems (such as the absorption of carbon dioxide) are of commercial importance. It has also been assumed in the past that for gas-phase controlled mass transfer, little increase in mass transfer rate could be obtained by adding a reactant to the liquid to remove the small liquid-phase resistance. This assumption has been shown to be incorrect earlier in this series (*16*) and by the unpublished work of Fellinger (*5*) on ammonia absorption in sulfuric acid, and Secor (*8*) on absorption of ammonia in boric acid solutions. This work indicated that gas-phase mass transfer coefficients, even for normally gas-phase controlled systems, could be improved up to several hundred percent by the use of a liquid-phase reactant.

In order to model the system, it is necessary to develop a sound basis for the assumption that a system is gas-phase controlled and then find some sound data with which to test the model.

The variation of gas- and liquid-phase resistance with flow rates for absorption with no reaction may be obtained from Equations (2) and (3), developed and substantiated by Shulman et al. (*15*) and by Shulman and Margolis (*12*):

$$\left[\frac{k_g M_g P_{BM}}{G}\right]\left[\frac{u_g}{\rho_g D_g}\right]^{2/3} = 1.915\left[\frac{D_p G}{\mu_g(1-\epsilon)}\right]^{-.036} \tag{2}$$

$$\left[\frac{k_l D_p}{D_l}\right] = 25.1\left[\frac{D_p L}{\mu_l}\right]^{0.45}\left[\frac{\mu_l}{\rho_l D_l}\right]^{0.5} \tag{3}$$

The percent resistance in the gas phase may be obtained from

$$\frac{100/k_g}{\frac{1}{k_g}+\frac{H}{k_l}}$$

where H is Henry's law constant. By inserting the physical properties of the gas, liquid, and packing for the ammonia-water system at 72°F., we may obtain the gas-phase resistance as percent of total for absorption of ammonia into water in a column of 0.5-in. Raschig rings. This is plotted in Figure 1. Area A shows the region investigated by Secor and Southworth (9), who found 77% of the resistance to be in the gas phase. Dwyer and Dodge (3) did work in regions B and C and found the gas phase to contain from 70 to 90 and from 75 to 80% of the gas phase resistance, respectively.

For nominal industrial flow rates of $G \geq 250$ lb./(hr.)(sq.ft.) and $L \geq 1{,}000$ lb./(hr.)(sq.ft.) for this system, the gas phase contains at least 90% of the total resistance, so this system may be considered to be gas-phase controlled.

The overall mass transfer coefficient $K_g a$ for low concentration systems is usually calculated from the equation

$$K_g a = \frac{G}{MZ\underline{P}} \frac{y_1 - y_2}{\Delta y_{lm}} \qquad (4)$$

where the log mean driving force Δy_{lm} is

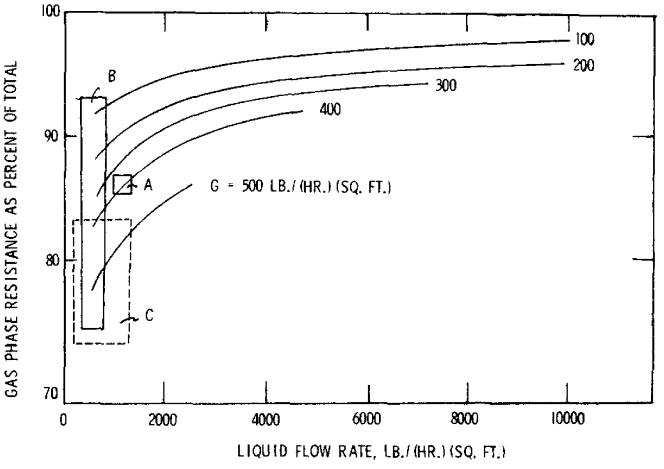

Fig. 1. Gas-phase resistance versus liquid and gas flow rates for ammonia-air-water systems in 0.5-in. Raschig rings.

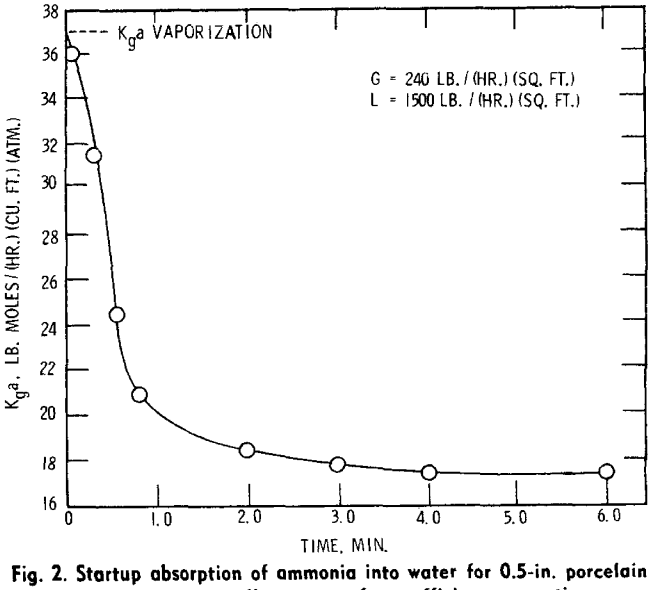

Fig. 2. Startup absorption of ammonia into water for 0.5-in. porcelain Raschig rings. Overall mass transfer coefficient versus time.

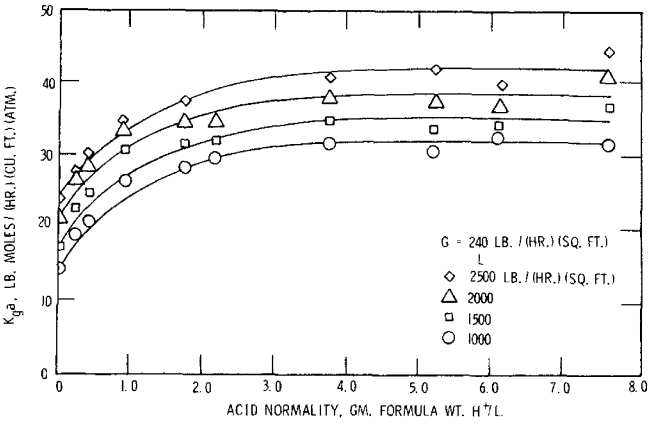

Fig. 3. Steady state absorption with liquid-phase reaction for ammonia-sulfuric acid system. Overall mass transfer coefficient versus acid normality for 0.5-in. porcelain Raschig rings.

$$\Delta y_{lm} = \frac{(y - y^*)_1 - (y - y^*)_2}{\ln \dfrac{(y - y^*)_1}{(y - y^*)_2}}$$

This equation assumes steady state countercurrent flow; that the system is dilute; that G, $K_g a$, and $\underline{P}$ are constant down the column; and, linear equilibrium and operating lines. If $y >> y^*$ or the average gas concentration is much greater than the average equilibrium pressure, Equation (4) reduces to the simpler form

$$K_g a = \frac{G}{MZ\underline{P}} \ln (y_1/y_2) \qquad (5)$$

Equations (5) and (4) are referred to as the steady state packed-column mass transfer equations, and the overall mass transfer coefficients may be calculated from these and values of the gas phase concentrations, flow rates, and column height.

Much mass transfer data for absorption with and without reaction was taken for the ammonia-water and ammonia-sulfuric acid systems. Some of these data are tabulated in Appendix A.* The first set of results, illustrated in Figure 2, is a transient or startup curve of $K_g a$ versus time for the case of absorption with no reaction. The curve illustrated is for absorption of ammonia into water for a bed 4 in. wide and 8 in. high, packed with 0.5-in. porcelain Raschig rings for which the values of $K_g a$ were calculated using the steady state Equation (4) to approximate the transient response. This is quantitatively justified in Appendix B.* If the $K_g a$ versus time curve is extrapolated to $t = 0$, one obtains a number very close to $K_g a$ for vaporization of pure ammonia [obtained by vaporizing water in the packed column and correcting the $K_g a$ by the factor $(D_{NH_3}/D_{H_2O})^{2/3}$], which, under these conditions, is around 37. lb.-moles/(hr.)(cu.ft.)(atm.). Also, for large times the curve levels off at the steady state value or $K_g a$ for absorption ($K_g a_{abs}$). Other packed-column transient curves for similar systems are similar in shape, can be extrapolated to $K_g a_{vap}$ for $t = 0$, and approach $K_g a$ for absorption for large t.

Illustrated in Figure 3 is a plot of $K_g a$ versus acid normality for steady state absorption of ammonia into sulfuric acid in a bed 4 in. wide by 8 in. high packed with 0.5-in. porcelain Raschig rings. Saal (7) showed that the ammonia-acid reaction

* Appendices have been deposited as document No. 01384 with the ASIS and may be obtained for $2.00 for photoprints or $5.00 for 35 mm. microfilm.

$$NH_3 + H^+ \underset{k_r}{\rightarrow} NH_4^+$$

is immeasurably rapid [$k_r >> 10^9$ l/(g.-mole)(sec.)]. Emerson et al. (4) found $k_r = 4.3 \times 10^{10}$ liter/(g.-mole)(sec.). For a strong acid and moderately strong base, we may assume that the reaction goes to completion. Therefore the ammonia-sulfuric acid reaction may be considered to be instantaneous and to go to completion. Curves are shown for liquid rates of 1,000, 1,500, 2,000, and 2,500 lb./(hr.)(sq.ft.). These curves start off for zero acid normality at K_ga for absorption and rise to values close to K_ga for vaporization at high (5 normal) acid concentrations. For example, for G = 240 lb./(hr.)(sq.ft.) and L = 1,500 lb./(hr.)(sq.ft.), conditions close to those of Figure 2, the curve rises from a value for K_ga of 17 lb.-moles/(hr.)(cu.ft.)(atm.) to an average K_ga of 35 lb.-moles/(hr.)(cu.ft.)(atm.), which is close to the K_ga for vaporization of 37 lb.-moles/(hr.)(cu.ft.)(atm.) considering the precision of the data.

This set of data illustrates why the penetration theory fails for gas-phase controlled absorption with liquid-phase reaction. The penetration theory would predict that the addition of a large amount of reactant to the liquid would negate all absorbed material, thereby wiping out most of the liquid-phase resistance. The mass transfer rate should increase accordingly. So, for this case, where liquid-phase resistance constitutes 10% of the total resistance, the mass transfer coefficient should rise by up to 10% with increasing liquid reactant concentration. But the mass transfer coefficient rises by more than 100%. This illustrates the need for a new model for packed columns.

Illustrated in Figure 4 is a plot of K_ga versus y_1 (inlet gas-phase mole fraction of the ammonia) for absorption of ammonia into sulfuric acid for G = 245 lb./(hr.)(sq.ft.), L = 1,500 lb./(hr.)(sq.ft.), and a 1.8 normal acid feed stream. This curve can be extrapolated to a value around 39 lb.-moles/(hr.)(cu.ft.)(atm.) for $y_1 = 0$, which is again close to K_ga for vaporization of 37 lb.-moles/(hr.)(cu.ft.)(atm.) considering the extrapolation. For large values of y_1 the curves seem to drop off and asymptotically approach K_ga for absorption in water of around 17 lb.-moles/(hr.)(cu.ft.)(atm.) as in Figure 2. As can also be seen from Figure 4, the K_ga for absorption with no reaction does not change appreciably with y_1.

The results shown in Figures 2 and 4 were obtained by using a column of unusual design. This column was specially constructed to minimize end effects. The liquid feed was first split equally among feeder tubes which put the liquid directly onto the packing with no splashing or fog formation. This could be observed through the glass-walled 4-in. diam. column. Small wires in the form of an inverted V led the liquid from feeder tubes to the surface of the packing with no splashing. The liquid drained out of the packing through a series of downcomers into a covered sump below, thereby eliminating as much as possible any contact of inlet gas and liquid. The gas feed entered into a chamber equipped with a series of risers which extended into the packing. The risers had roofs over them so no liquid could pass into the entering gas stream. The gas outlet was located about 2 ft. above the top of the packing. With this type of column, the end effect correction when averaged over gas and liquid flow rates covered was 0.76 for a packed bed 8 in. deep. The end effect correction was obtained by plotting K_ga versus $1/Z$ for two packing heights and extrapolating the curves to $1/Z = 0$ or $Z = \infty$. The end effect correction for an 8-in. deep bed is then $K_ga_{Z=\infty}/K_ga_{Z=8\text{ in.}}$. The same general trends have been shown by Fellinger (5), Sherwood (10), and Secor (8, 9).

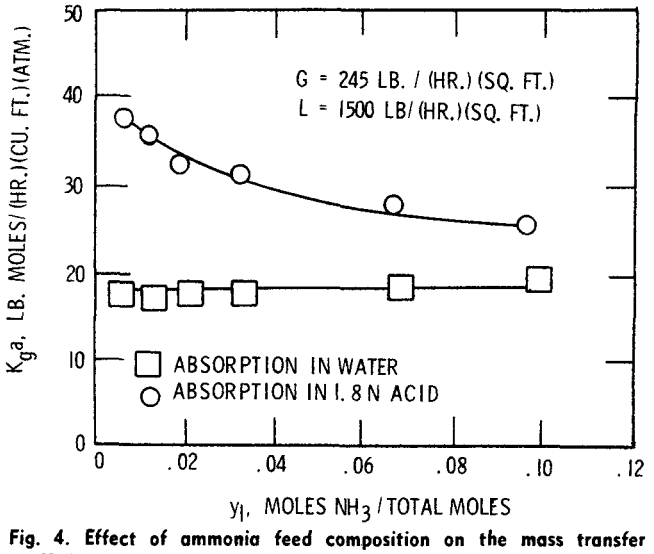

Fig. 4. Effect of ammonia feed composition on the mass transfer coefficient in water and acid. Overall mass transfer coefficient versus inlet gas concentration for 0.5-in. porcelain Raschig rings.

The observed variations in mass transfer rates can be explained qualitatively by means of the slow turnover in the pockets of fluid previously mentioned. Shulman and co-workers (14) have advanced the explanation that for the cases of vaporization and startup all parts of the wetted packing surface area are effective for mass transfer. However, for absorption at steady state, portions of the fluid, such as slow moving puddles inside rings, which are stagnant or nearly so, become saturated, thereby reducing mass transfer in these sections of the packing. In other words, the total wetted surface area is available for mass transfer in vaporization or at startup but, for steady state absorption, the effective area available for mass transfer is much less, due to stagnation of some parts of the fluid.

As the liquid-phase reactant concentration increases, the inlet reactant concentration increases and the pockets become more effective. For high reactant concentrations, almost all pockets will be effective and the mass transfer coefficients will be near those for vaporization. This concept is borne out by the experimental data.

Increasing inlet gas-phase concentrations result in decreasing mass transfer coefficients when a liquid reactant is used, because rapid saturation of semistagnant pockets counterbalances the beneficial effects of the reactant. In no case does the mass transfer coefficient fall below that observed for absorption without reaction.

The mass transfer phenomena presented in Figures 2, 3, and 4 and the discussion presented above suggest that any model which is to simulate a packed column successfully must take into account the distribution of the residence times of the different portions of the liquid phase. The recent work of Vivian and Schoenberg (17), employing a short wetted-wall column, proves there is no difference in the basic mass transfer mechanism for vaporization and absorption and reinforces the need for a model based on the distribution of the residence times of the liquid pockets in a packed column.

LIQUID DISTRIBUTION MODEL

After testing a variety of models we found the most suitable to be one which consisted of a number of continuous stirred-tank reactors (CSTR) in parallel with mass transfer to the exposed liquid surface, as illustrated in Figure 5. This model consists of N CSTR's in parallel having different residence times where the mass transfer rate

to each CSTR is proportional to the difference between the partial pressure of ammonia in the gas phase and the equilibrium pressure or back pressure of ammonia in the CSTR. First it is necessary to determine the way in which the liquid is distributed among the CSTR's.

In order for the model to approximate the empirical relationship

$$\frac{K_g a_{vap}}{K_g a_{abs}} = \frac{h_t}{h_o}$$

the liquid distribution would have to be such that about 4/5 of the liquid would go through one or two CSTR's while the rest of the liquid would be divided up among the remaining CSTR's. Also, one or two CSTR's would have to have relatively long residence times to make the $K_g a$ versus time curve drop off to steady state in about 3 min. It would be advantageous for design purposes to have the simplest distribution possible so that a minimum number of parameters need be correlated and used by the designer. A simple liquid distribution which gives this result is given by Equation (6), as plotted in Figure 6:

$$E_k = \frac{\alpha\,[B/(1-B)]}{1+\alpha\,[B/(1-B)]} \qquad (6)$$

where

$$B = \frac{k}{N}, \qquad fr_k = \frac{E_k}{\sum_{k=1}^{N} E_k}$$

Since L is in pounds per hour per square foot, the flow rate to the actual column is obtained by multiplying L by the column cross-sectional area in square feet. The volumetric rate of flow q_k to a reactor k is the weight rate of flow divided by the liquid density, or

$$q_k = fr_k \frac{LA}{\rho_l} \qquad (7)$$

For this application, α is less than 1.0. The advantage of using this distribution is its inherent simplicity. It takes little time to calculate the values of fr_k and only one parameter α need be correlated.

In order to fit the model to the experimental data available, a too large value of α was chosen (0.95) as a first guess and the steady state or $t = \infty$ value of $K_g a_M$ for the model for absorption with no reaction was calculated as in the following section (transient response). Then $K_g a_M$ was compared to $K_g a_{abs}$ and if there was a 1% difference or less, that value of α was used. If the difference was greater than 1%, then a next guess at α was calculated from

$$\alpha_2 = \alpha_1\,(K_g a_{abs}/K_g a_M)\ 0.96$$

Since the smaller $K_g a_{abs}$ is, the smaller α will have to be to satisfy the condition $K_g a_M = K_g a_{abs}$ at $t = \infty$. The factor 0.96 was used to make the iteration converge faster. Without the 0.96 factor it took up to 50 iterations to converge, whereas with the factor it took 10 iterations at most to converge to $K_g a_{abs}$. The factor 0.96 was found to make the system converge rapidly without undershooting the value of $K_g a_{abs}$ by more than 1%. This procedure determines a value of α and the liquid distribution to be used at a given gas and liquid rate.

TRANSIENT RESPONSE

A mass balance can now be written to calculate the ammonia concentration in a reactor for the transient case with no reaction. Assuming CSTR k in Figure 5 is thoroughly mixed and of constant volume with no reaction

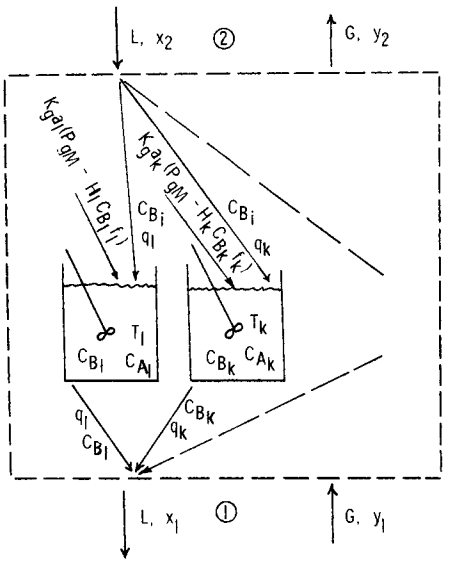

Fig. 5. Diagram of the model.

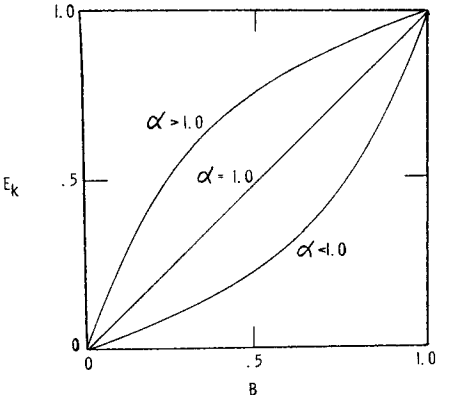

Fig. 6. Liquid distribution function.

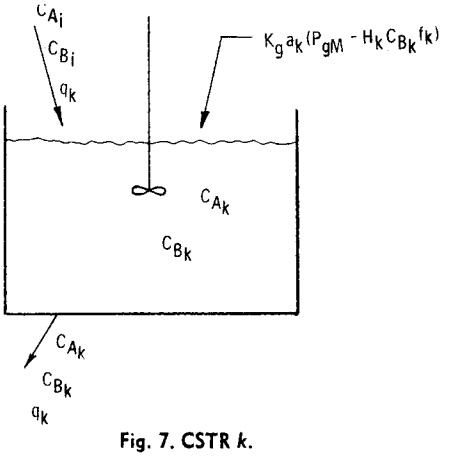

Fig. 7. CSTR k.

taking place, one can write a mass balance on ammonia around the CSTR as follows:

$$q_k C_{Bi} - q_k C_{Bk} + K_g a_k\,(P_{gM} - H_k C_{Bk} f_k) = \frac{d(v_k C_{Bk})}{dt}$$

and

$$K_g a_k = K_g a_{vap}\left[\frac{V}{N}\right], \qquad v_k = \frac{h_t V}{N}$$

with the assumption that the areas a_k and volumes v_k for all of the CSTR's are equal. This may be rearranged to obtain

$$\frac{dC_{Bk}}{dt} + \frac{1}{v_k}(K_g a_k H_k + q_k)C_{Bk} = \frac{1}{v_k}(K_g a_k P_{gM} + q_k C_{Bi})$$

Since H_k will vary with temperature and therefore with time, this equation must be solved as a first-order ordinary differential equation with variable coefficients to get

$$C_{Bk} = \frac{I_1 + \int_0^t \frac{K_g a_k P_{gM}}{v_k} e^{\int_0^t \frac{q_k}{v_k}\left(1 + \frac{K_g a_k H_k}{q_k}\right) dt} dt}{e^{\int_0^t \frac{q_k}{v_k}\left(1 + \frac{K_g a_k H_k}{q}\right) dt}}$$

At startup, $t = 0$ and, assuming that no ammonia is present in the liquid, $C_{Bk} = 0$, so $I_1 = 0$.

We may assume that the only way heat can be transferred out of a CSTR is through the effluent liquid stream. A heat balance may then be written around CSTR k as follows:

$$q_k \rho_l C_p (T_i - T_i)_k - q_k \rho_l C_p (T - T_i)_k + K_g a_k (P_{gM} - H_k C_{Bk} f_k)\Delta H = \frac{d(C_p T \rho_l v_k)}{dt} \quad \frac{d[C_p \rho_l v_k (T - T_i)_k]}{dt}$$

For

$$NH_{3\,g} \xrightarrow[18°C.]{} NH_{3\ \text{soln.}}$$

0.011 atm. 200 g.-moles H_2O

$\Delta H = 10{,}400$ B.t.u./lb.-mole

Assuming ρ_l and C_p are constant over the temperature range considered

$$\frac{d(T - T_i)_k}{dt} + \frac{q_k}{v_k}(T - T_i)_k = \frac{K_g a_k (P_{gM} - H_k C_{Bk} f_k)\Delta H}{C_p \rho_l v_k}$$

which can be solved as a first-order ordinary differential equation with variable coefficients (H_k varies with T), the solution of which is

$$(T - T_i)_k = \frac{I_2 + \int_0^t \frac{K_g a_k (P_{gM} - H_k C_{Bk} f_k)\Delta H}{C_p \rho_l v_k} e^{\int_0^t \frac{q_k}{v_k} dt} dt}{e^{\int_0^t \frac{q_k}{v_k} dt}} \tag{9}$$

At $t = 0$, $(T - T_i)_k = 0$, so $I_2 = 0$. Also, q_k/v_k is assumed to remain constant with time so that Equation (9) reduces to

$$(T - T_i)_k = \frac{\int_0^t \frac{K_g a_k (P_{gM} - H_k C_{Bk} f_k)\Delta H}{C_p \rho_l v_k} e^{\frac{q_k}{v_k} t} dt}{e^{\frac{q_k}{v_k} t}} \tag{10}$$

The Henry's law constant H in

$$P = H C f \tag{11}$$

may be calculated by a correlation developed by Kowalke et al. (6) and given by Chilton et al. (2) as

$$\log P/m = 4.699 - 1922/T \tag{12}$$

where P is the partial pressure of ammonia, m is the ammonia concentration in solution, f is the ammonia activity coefficient, and T is temperature. The value of $P/m = H$ may be converted to engineering units of atmosphere per pound-moles per cubic foot by dividing by 0.0624. This correlation is stated to hold for ammonia concentrations up to 4.5 g.-moles/liter and over the temperature range of 50° to 160°F. The ammonia activity coefficient f approaches unity as the salt concentration in the solution approaches zero and would be 1.0 for this case.

The total mass transfer rate in the model at any time is

$$\sum_{k=1}^{N} K_g a_k (P_{gM} - H_k C_{Bk} f_k)$$

This may be corrected to 1 cu.ft. of packing by dividing by the column volume V. This expression can then be set equal to some overall mass transfer coefficient for the model $K_g a_M$ times the log mean driving force Δy_{lm} to obtain

$$K_g a_M \underline{P}\,\Delta y_{lm} = \frac{\sum_{k=1}^{N} K_g a_k (P_{gM} - H_k C_{Bk} f_k)}{V} \tag{13}$$

where

$$P_{gM} = \underline{P}\,\Delta y_{lm}$$

The Δy_{lm} term is the log mean driving force and, assuming $y_2^* = 0$ (pure water feed) and $y_1^* << y_1$, is

$$\Delta y_{lm} = \frac{y_1 - y_2}{\ln (y_1/y_2)} \tag{14}$$

The driving force P_{gM} is, for the conditions of pure liquid feed and negligible bulk concentration of absorbate, the log mean partial pressure of absorbate in the column. The model thus assumes this log mean partial pressure of absorbate to exist above all of the CSTR's. This was done to duplicate as closely as possible the general packed-column mass transfer equation which can be rearranged to give

$$K_g a \underline{P}\,\Delta y_{lm} = \frac{G}{Z M}(y_1 - y_2) \tag{15}$$

There is little difference between the right-hand sides of Equations (13) and (15) since the residence time of the gas in the small experimental column was less than 1 sec. For a larger column with larger residence time an accumulation term might have to be introduced into Equation (13) and the equation developed in Appendix B* used in place of the steady state packed-column equation.

The integrals may be approximated by the trapezoidal rule. The time increment should be chosen small enough so that the solutions for C_{Bk} and T do not depend on the size of the increment chosen.

The solution for startup was obtained as follows. Using the previously determined α and the liquid distribution, and inserting $K_g a = K_g a_{abs}/F$ and y_1 into Equation (5), one obtains a value of y_2 at steady state. Using y_1 and y_2 in Equation (14), one determines a value of Δy_{lm}. A solution of $(T - T_i)_k$ versus time was assumed as zero for

* See footnote on page 632.

each CSTR k. Equation (8) was solved, giving a solution of C_{Bk} versus time for each CSTR. The solution of the total mass transfer coefficient versus time could be obtained from Equation (13). This is used with Equation (5) and Equation (14) to obtain a solution of Δy_{lm} and P_{gM} with time. Now Equation (9) can be solved using the previously assumed solution of H_k versus time to obtain a new approximation of T versus time for each CSTR. A new solution of H_k versus time can be found from Equation (12). Then this new result can be used with Equation (8) to give a new solution of C_{Bk} versus time. Using the new values of P_{gM}, H_k, and C_{Bk}, one can use Equation (13) to obtain a new solution of the overall mass transfer coefficient and the process repeated.

It was found that the solutions of T versus time changed by 0.5°F. between the second and third iterations and changed less than 0.05°F. between the third and fourth iterations, so these equations were solved using four iterations.

DYNAMIC RESPONSE

A simple approximation to the effect of controlled cycling may be obtained by assuming that pulse widths are small and that total washout and renewal of each CSTR occurs at each liquid cycle. This is equivalent to the startup problem covered in the section on Transient Response where the problem starts over at every pulse. The average total $K_g a_M$ may be obtained from

$$\text{average } K_g a_M = \frac{\int_{t_1}^{t_2} K_g a_M \, dt}{t_2 - t_1}$$

using the trapezoidal rule to approximate the integral. The time intervals should be chosen small enough so that the solution of C_{Bk} and T versus time do not depend on the size of the interval.

STEADY STATE WITH LIQUID-PHASE REACTION

If one assumes that a reaction, for instance the reaction of ammonia with sulfuric acid

$$2NH_3 + H_2SO_4 \rightarrow (NH_4)_2SO_4$$

is instantaneous and goes to completion, a mass balance on ammonium hydroxide may be written around the CSTR in Figure 7 as

$$q_k C_{Bi} + K_g a_k (P_{gM} - H_k C_{Bk} f_k) - C_{Ai} q_k - C_{Bk} q_k = 0 \tag{16}$$

Assuming $C_{Bi} = 0$ or that there is no ammonia in the inlet acid stream, one can rearrange Equation (16) to give

$$C_{Bk} = \frac{(K_g a_k P_{gM} - C_{Ai} q_k)}{(q_k + K_g a_k H_k f_k)} \tag{17}$$

which can be solved for the concentration of free ammonia or unreacted ammonium hydroxide in a reactor where all of the acid is reacted. If C_{Bk} is negative, then

$$q_k C_{Ai} > K_g a_k P_{gM}$$

or there is more acid flowing into the reactor than can be neutralized, so all of the ammonia that enters the solution reacts and there is an excess of acid in the reactor. For this case, C_{Bk} would be zero and the acid concentration C_{Ak} in the exiting stream may be obtained from the acid mass balance

$$C_{Ai} q_k - C_{Ak} q_k - K_g a_k (P_{gM} - H_k C_{Bk} f_k) = 0$$

as

$$C_{Ak} = (C_{Ai} q_k - K_g a_k P_{gM})/q_k \tag{18}$$

Now the temperature change and Henry's law correction in a CSTR for absorption of ammonia into sulfuric acid must be calculated. The heat generated Q would be

$$Q = K_g a_k (P_{gM} - H_k C_{Bk} f_k) \Delta H_r$$

where ΔH_r is the heat of solution plus reaction per pound-mole of ammonia absorbed for

$$K_g a_k (P_{gM} - H_k C_{Bk} f_k) < C_{Ai} q_k$$

Where there is excess acid in the CSTR and $C_{Bk} = 0$ and

$$Q = C_{Ai} q_k \Delta H_r + (K_g a_k (P_{gM} - H_k C_{Bk} f_k) - C_{Ai} q_k) \Delta H$$

for

$$K_g a_k (P_{gM} - H_k C_{Bk} f_k) > C_{Ai} q_k$$

there is excess ammonia in the CSTR and $C_{Bk} = 0$. Again assuming that the only way heat may be lost from a CSTR is through the effluent liquid stream, one can write a steady state heat balance around CSTR k

$$q_k \rho_l C_p (T_i - T_i)_k - q_k \rho_l C_p (T - T_i)_k + Q = \frac{d(C_p T \rho_l v_k)}{dt} = 0$$

which can be solved for the temperature rise $(T - T_i)_k$

$$(T - T_i)_k = \frac{Q}{q_k \rho_l C_p} \tag{19}$$

The concentration of ammonium sulfate salt in CSTR k will have an effect on ammonia partial pressure since $f \neq 1.0$. A correlation of f versus ammonium sulfate concentration may be obtained for concentrations up to 3 g.-moles/liter (corresponding to 6 normal sulfuric acid totally reacted) and temperatures of from 25° to 98°C. for the equation

$$P_{NH_3} = H_k C_{Bk} f_k \tag{20}$$

from the results of Benoit (*1*)

$$\log_{10} f_k = K_k C_{k(NH_4)_2SO_4} \tag{21}$$

where $C_{k(NH_4)_2SO_4}$ is the concentration of ammonium sulfate in gram-moles per liter. Two values are given for K

$$K = 0.134 \qquad T = 25°C.$$

$$K = 0.124 \qquad T = 60°C.$$

Equation (20) is presented incorrectly in Benoit's paper. Equations (20) and (21) were found to check with a plot of data given in Benoit's paper (*1*). The ammonium sulfate concentration in reactor k can be calculated from

$$C_{k(NH_4)_2SO_4} = \frac{K_g a_k (P_{gM} - H_k C_{Bk} f_k)}{2 q_k (0.0624)} \text{ g.-moles/liter}$$

for the case of

$$K_g a_k (P_{gM} - H_k C_{Bk} f_k) > C_{Ai} q_k$$

or where the ammonia is entering the CSTR at a faster rate than the acid. This is the only case of interest, since for

$$K_g a_k (P_{gM} - H_k C_{Bk} f_k) < C_{Ai} q_k$$

or acid entering at a faster rate, there would be no ammonia in the solution or $C_{Bk} = 0$ and the $H_k C_{Bk} f_k$ term would disappear. A straight line was drawn between the two given values of K to obtain the temperature correlation

$$K_k = -0.000286 [22.0 + 0.555 (T - T_i)_k] + 0.141$$

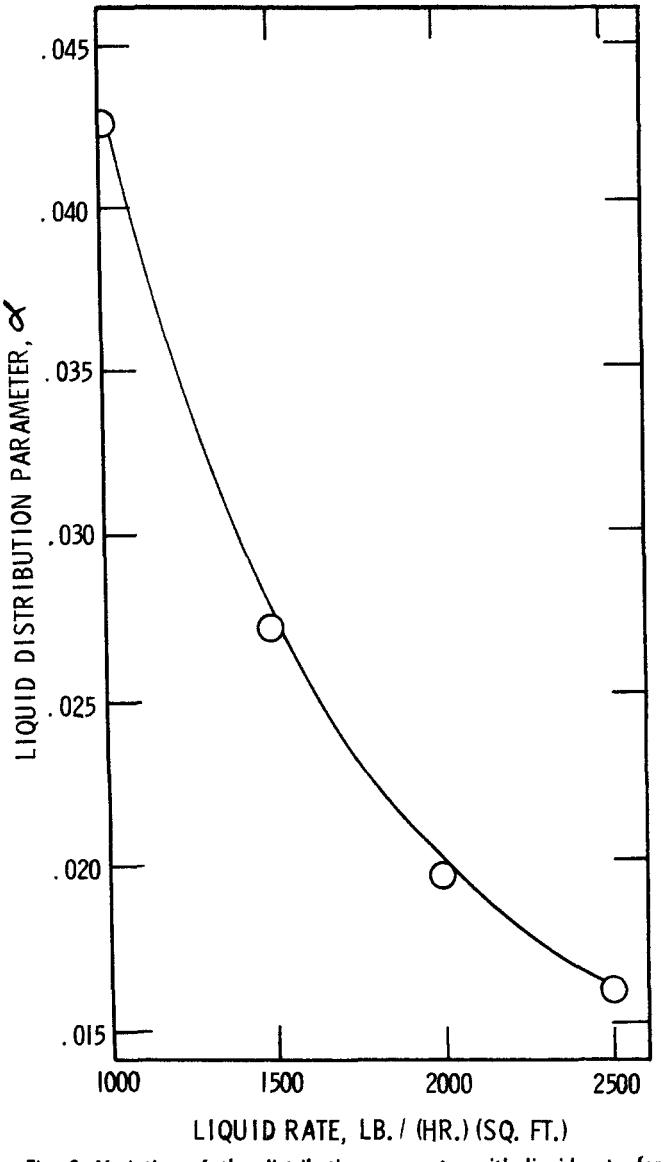

Fig. 8. Variation of the distribution parameter with liquid rate for the model.

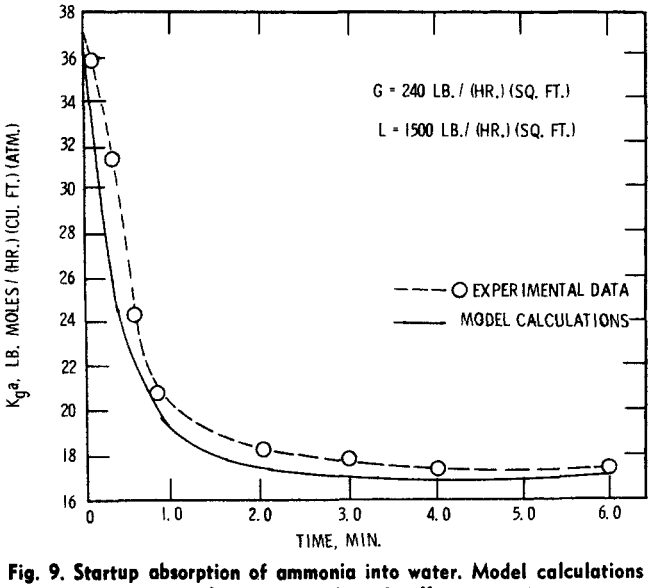

Fig. 9. Startup absorption of ammonia into water. Model calculations compared with experimental results. $K_g a$ versus time.

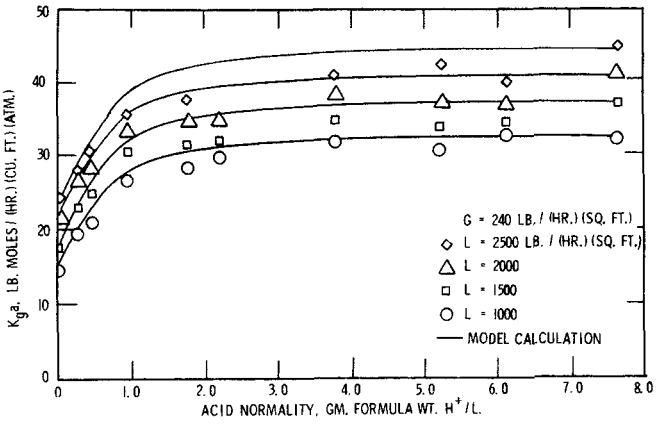

Fig. 10. Effect of inlet acid concentration on overall mass transfer coefficient for model compared with experimental results. $K_g a$ versus acid normality.

in terms of $(T - T_i)_k$, the temperature rise of CSTR k from 72°F. (22°C.).

The method of solution of the reaction problem is as follows. For the first iteration, $(T - T_i)_k$ is assumed to be zero (all CSTR's at ambient temperature) and f_k is assumed to be 1.0 (zero salt concentration). Assuming y_2 for steady state absorption for no reaction, a Δy_{lm} is calculated and the ammonium concentrations C_{Bk} are calculated from Equation (8). The overall mass transfer coefficient for the model $K_g a_M$ can be calculated from Equation (13). Now a new guess at $(T - T_i)_k$ from (19) and salt concentration will give a new guess at H_k and f_k from (12) and (21). Also, a new guess at y_2 may be obtained from Equation (5) using $K_g a = K_g a_M / F$, where $F = 0.76$. This new y_2 is compared with the previous value of y_2 and if they differ by more than 1% the procedure is repeated using the new value of y_2. This converges in four iterations.

DISCUSSION OF RESULTS

The systems of equations for a model consisting of 10 CSTR's in parallel were solved on an IBM 360 model 44 digital computer. The experimental transient response curve was used to give values of $K_g a_{abs}$ and $K_g a_{vap}$ for the model. The value of $K_g a_{abs}$ for steady state at $L = 1{,}500$ lb./(hr.)(sq.ft.) was taken as the value at which the transient or startup curve leveled off, 17 lb.-moles/(hr.)(cu.ft.)(atm.). The value of $K_g a_{vap}$ was obtained by extrapolating the transient curve to $t = 0$ to obtain a value of 37 lb.-moles/(hr.)(cu.ft.)(atm.). The transient curve must be experimentally determined on a small column with small residence time or corrected as described in Appendix B.* The values of $K_g a_{vap}$ and $K_g a_{abs}$ at other liquid flow rates were determined from the following equations:

$$K_g a_{vap_{L,G}} = 37 \frac{\text{lb.-moles}}{(\text{hr.})(\text{cu.ft.})(\text{atm.})} \left[\frac{L}{1{,}500}\right]^{0.33} \left[\frac{G}{240}\right]^{0.69}$$

$$K_g a_{abs_{L,G}} = 17 \frac{\text{lb.-moles}}{(\text{hr.})(\text{cu.ft.})(\text{atm.})} \left[\frac{L}{1{,}500}\right]^{0.33} \left[\frac{G}{240}\right]^{0.69}$$

which come from the equation $k_g a \propto L^{0.33} G^{0.69}$, which is illustrated by Shulman et al. (*16*). It has been found by other researchers (*3, 11*) that an equation of this general

* See footnote on page 632.

type holds for gas-phase controlled absorption. The values of y_1 were taken from the experimental data for each point involved. The total liquid holdup may be obtained from Shulman et al. (*16*) and, for 0.5-in. Raschig rings at $G =$ 240 lb./(hr.)(sq.ft.), may be represented as a straight line

$$h_t = 0.145 \times 10^{-4}L + 0.0515$$

The variation of the distribution parameter α with liquid flow rate L is shown in Figure 8. The smooth curve makes it easy to interpolate to find a value of the liquid distribution parameter at some intermediate flow rate. The startup curve of $K_g a_M$ versus time is shown in Figure 9 along with

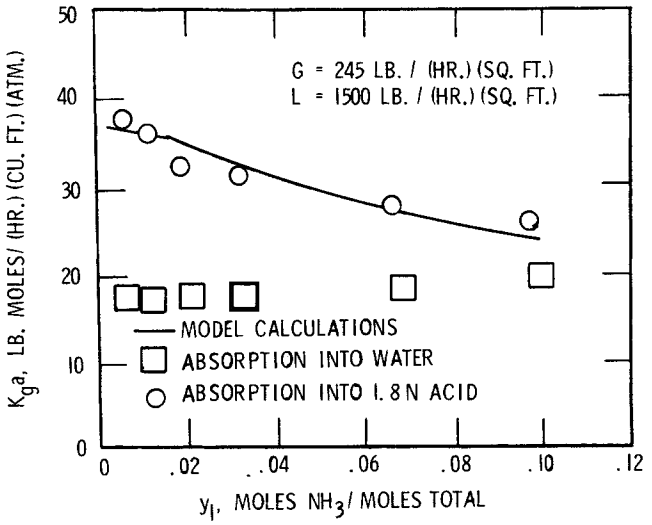

Fig. 11. Variation of the mass transfer coefficient with inlet gas concentration for absorption into water and acid for model and experimental data.

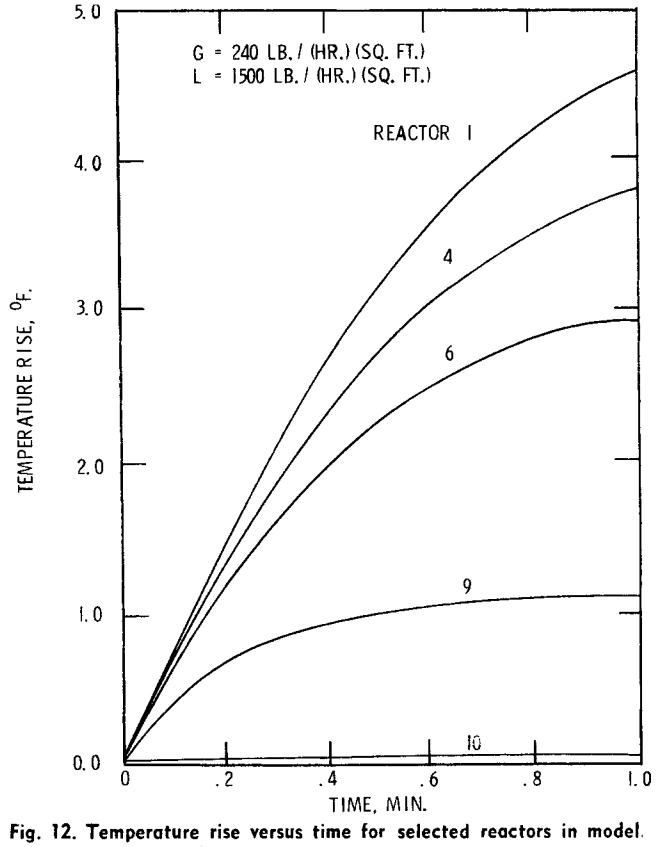

Fig. 12. Temperature rise versus time for selected reactors in model. Ammonia absorption in water.

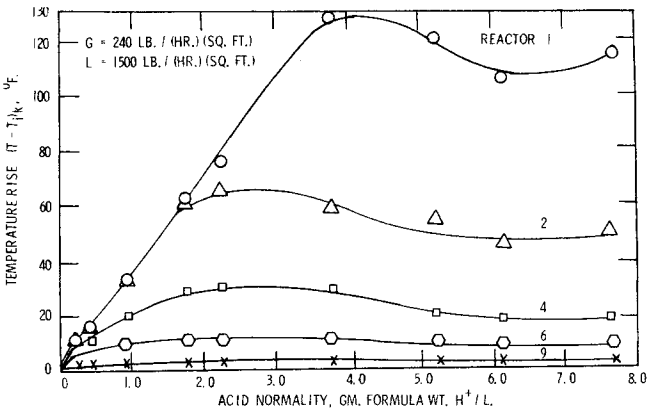

Fig. 13. Temperature rise versus acid normality for selected reactors in model. Absorption of ammonia into sulfuric acid.

the experimental results for comparison. The difference between solutions for 0.1 and 0.05 min. increments was 2.0%, while the difference for increments of 0.05 and 0.025 min. was negligible. An increment size of 0.1 min. was used for the solution shown. The maximum difference between model and experimental results is about 20% over a small region. The variation of $K_g a_M$ with inlet acid normality is shown in Figure 10 compared to the experimental results. There is a maximum difference of 15% between model and experimental results, with most of the differences well under 10%. Figure 11 shows the variation of $K_g a_M$ with inlet gas concentration for 1.8 normal acid feed. This curve shows a maximum difference of 5% between predicted and experimental results.

The residence times of the CSTR's vary from 0.01 to 6 min. Doubling the number of CSTR's from 10 to 20 raises the $K_g a_M$ versus acid normality curve by 3% in some places and the $K_g a_M$ versus time and $K_g a_M$ versus y_1 curves by 0 to 2%. This is probably due to using the same value for α for 20 as for 10 reactors. The value of α would probably change slightly with the number of reactors used.

The first guess at y_2 for the model was obtained from Equation (5) using the steady state value of $K_g a_{abs}$ for no reaction and an average end effect correction of 0.76 to be consistent with the experimental data. Now

$$P_{gM} = \underline{P}\,\Delta y_{lm}$$

where Δy_{lm} was calculated assuming $y_2^* = 0$ (pure water feed) and $(y - y^*)_1 = y_1$ since $y_1^* << y_1$.

A plot of temperature rise versus time for $G = 240$ and $L = 1{,}500$ lb./(hr.)(sq.ft.) is shown in Figure 12 for CSTR's 1, 4, 6, 9, and 10 when 10 CSTR's are used. This is for the absorption of ammonia into water with no liquid-phase reaction. A 5°F. temperature rise will increase H by approximately 15%.

A plot of temperature rise (from 72°F.) versus acid normality for $G = 240$ and $L = 1{,}500$ lb./(hr.)(sq.ft.) is shown in Figure 13 for reactors 1, 2, 4, 6, and 9. This is for the steady state absorption of ammonia into sulfuric acid with liquid-phase reaction. It may be noted that the temperature in CSTR 1 rises to 72 + 128 = 200°F., which is 40°F. over the range of the H versus T correlation (12) given by Kowalke et al. In the absence of any high temperature correlation Equation (12) had to be used for the higher temperatures. Only CSTR 1 exceeds the temperature range of Equation (12). Over an inlet acid normality of 2.0 all $C_{Bk} \cong 0$, so that $P_{gM} >> H_k C_{Bk}$ for CSTR 1 and thus the $H_k C_{Bk}$ term would drop out. The effect on $K_g a_M$ of running over the temperature limits for Equation (12) is thus assumed negligible. Correlations (20) and

(21) for partial pressure of ammonia over an ammonium sulfate solution are stated by Benoit to hold to 208°F.

For both the cases of reaction and no liquid-phase reaction, the temperature rise is greatest in CSTR 1, which has the smallest throughput and largest residence time. This is to be expected since the only means of transferring heat out of the reactors is assumed to be through the effluent liquid stream. The largest temperature rise would occur in a stagnant pocket which has no liquid throughput.

For the dynamic solution it was found that the difference in the solutions of $K_g a_M$ versus time for increments of 0.10 and 0.05 min. was 2.0%. There was no difference in solutions between time increments of 0.050 and 0.025 min.

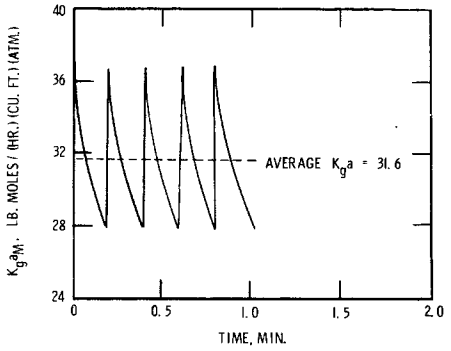

Fig. 14. The response of model to liquid cycling. Overall mass transfer coefficient versus time. Period = 0.2 min.

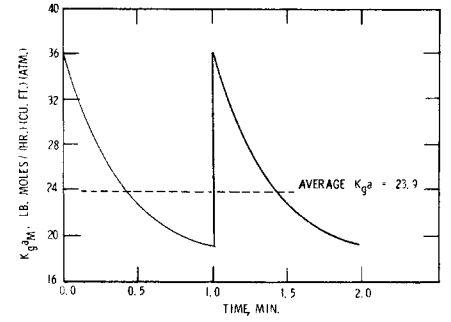

Fig. 15. The response of model to liquid cycling. Overall mass transfer coefficient versus time. Period = 1.0 min.

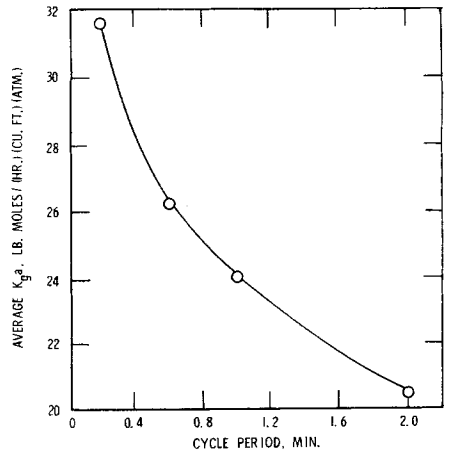

Fig. 16. Average overall mass transfer coefficient as a function of cycle period for model. Absorption of ammonia into water in 0.5-in. Raschig rings.

The dynamic solutions shown were obtained using a time increment of 0.050 min. and flow rates of $G = 240$, $L = 1{,}500$ lb./(hr.)(sq.ft.). Between iterations 2 and 3 some values of $K_g a_M$ changed by 7%, whereas the difference between iterations 3 and 4 was 0.2% at most. The solutions shown were obtained using 4 iterations. Dynamic solutions were obtained for pulse periods of 0.2, 0.6, 1.0, and 2.0 min., with average total mass transfer coefficients of 31.6, 26.1, 23.9, and 20.5 lb.-moles/(hr.)(cu.ft.)(atm.), respectively. Two of the dynamic solutions are shown in Figures 14 and 15 for pulse periods of 0.2 and 1.0 min. A plot of average $K_g a_M$ versus cycle period is shown in Figure 16. It is apparent that the mass transfer rate rises with decreasing cycle period or increasing cycle frequency and that the efficiency may rise as much as 100% for rapid cycling of the model. This is qualitatively in accord with the sparse experimental results in the literature. This analysis would most closely correspond to controlled cycling since we are assuming that the mechanism is one of emptying and replenishment of liquid-phase pockets.

The model and treatment shown should be applicable to any packed column of any size, provided it is operated near loading with proper gas and liquid distribution and provided some experimental data for the packing are available and have been properly end effect corrected. The steady state results are directly applicable to any size column with an instantaneous liquid-phase reaction going to completion. For a reaction that is not instantaneous and/or does not go to completion, one would have to write ion balances around the reactors and equilibrium expressions for the products. For a dynamics study of a large column one would have to use the transient equation developed in Appendix B* instead of Equation (5) to find successive guesses for the curve y_2 versus time, due to the much larger volume or gas-phase accumulation term.

SUMMARY AND CONCLUSIONS

Previously it had been difficult to predict mass transfer rates for gas-phase controlled absorption with liquid-phase reaction in packed columns for different inlet liquid reactant and inlet gas concentrations. The problem existed in both the use of some consistent experimental data and in the description of a model to simulate the mass transfer.

A model consisting of 10 continuous stirred-tank reactors in parallel has been proposed. A distribution is presented which uses one parameter to determine the liquid distribution within the model.

The model successfully correlates all responses within 20%, most within 10%, including those of $K_g a$ versus time for no reaction, $K_g a$ versus inlet acid normality, and $K_g a$ versus inlet gas concentration for the liquid-phase reaction for the systems ammonia-water and ammonia-sulfuric acid. It also explains the increase in mass transfer rate obtained by controlled cycling.

It is now possible, knowing the desired y_1 and the $K_g a$ for steady state absorption and vaporization for a given system, to predict the value of $K_g a$ and the column height Z through Equation (4) for any time at startup for absorption without reaction and for any liquid-phase reactant concentration and inlet gas concentration for steady state absorption with reaction. No quantitative data are available tc compare with the dynamic results. However, the dynamic results qualitatively follow some reported results. This has been shown to hold for the systems ammonia-water and ammonia-sulfuric acid and there is no reason to believe that this analysis would not work with other systems for gas-phase controlled absorption.

* See footnote on page 632.

ACKNOWLEDGMENT

The authors acknowledge support of this work by the Atomic Energy Commission under Contract No. AT(30-1)-1463. W. G. Mellish was supported by a National Science Foundation Cooperative Fellowship and a National Defense Education Act Fellowship during part of this work.

NOTATION

a = effective interfacial area, sq.ft./cu.ft.
A = column cross-sectional area, sq.ft.
B = k/N
C_{Ai} = inlet acid [H^+] concentration to reactor, lb.-moles/cu.ft.
C_{Ak} = acid concentration of liquid in and effluent from reactor k, lb.-moles/liter
C_{Bi} = inlet NH_4OH concentration to reactor, lb.-moles/cu.ft.
C_{Bk} = concentration of NH_4OH in and effluent from reactor k, lb.-moles/cu.ft.
C_p = heat capacity of liquid, B.t.u./(lb.)(°F.)
D = diffusivity, sq.ft.
D_p = diameter of a sphere possessing the same surface area as a piece of packing, ft.
E = $\alpha[B/(1-B)]/[1+\alpha\{B/(1-B)\}]$
F = column end effect correction factor
f_k = activity coefficient
fr_k = fraction of liquid going to reactor k
G = gas flow rate, lb./(hr.)(sq.ft.)
G^* = gas flow rate of inerts, lb./(hr.)(sq.ft.)
h_o = operating liquid holdup, cu.ft./cu.ft.
h_s = static liquid holdup, cu.ft./cu.ft.
h_t = total liquid holdup, cu.ft./cu.ft.
H_k = Henry's law constant for reactor k, atm./(lb.-mole)(cu.ft.)
ΔH = heat of solution of active gas in pure liquid, B.t.u./lb.-mole
ΔH_r = heat of solution plus reaction of active gas in liquid with reactant, B.t.u./lb.-mole
I = constants of integration
K_g = gas-phase mass transfer coefficient, lb.-moles/(hr.)(sq.ft.)(atm.)
k_l = liquid-phase mass transfer coefficient, lb.-moles/(hr.)(sq.ft.)(atm.)
k_g = overall gas-phase mass transfer coefficient, lb.-moles/(hr.)(sq.ft.)(atm.)
$K_g a_{abs}$ = overall mass transfer coefficient for absorption, lb.-moles/(hr.)(cu.ft.)(atm.)
$K_g a_k$ = particular reactor overall mass transfer coefficient for reactor k, lb.-moles/(hr.)(atm.)
$K_g a_M$ = total mass transfer coefficient for the model, lb.-moles/(hr.)(cu.ft.)(atm.)
$K_g a_{vap}$ = overall mass transfer coefficient for vaporization, lb.-moles/(hr.)(cu.ft.)(atm.)
L = liquid flow rate, lb./(hr.)(sq.ft.)
L^* = liquid flow rate of inerts, lb./(hr.)(sq.ft.)
M_g = average gas molecular weight, lb./lb.-mole
M_l = average liquid molecular weight, lb./lb.-mole
N = number of CSTR's in model
P = average column pressure, atm.
$\overline{P_a}$ = atmospheric pressure
P_c = pressure drop across column
P_{gM} = column log mean partial pressure of active in gas, atm.
q_k = liquid throughput to reactor k, cu.ft./hr.
Q = heat generated, B.t.u./hr.
t = elapsed time, hr.
T = temperature, °F.
T_i = initial and reference temperature, °F.
V = volume of simulated column, cu.ft.
v_k = volume of reactor k, cu.ft.
x_1 = liquid outlet mole fraction active, lb.-moles active/lb.-moles total
x_2 = liquid inlet mole fraction active, lb.-moles active/lb.-moles total
X_1 = liquid outlet mole ratio active, lb.-moles active/lb.-moles inert
X_2 = liquid inlet mole ratio active, lb.-moles active/lb.-moles inert
X_t = liquid-phase mole ratio active at top of differential section, lb.-moles active/lb.-moles inert
X_b = liquid-phase mole ratio active at bottom of differential section, lb.-moles active/lb.-moles inert
y^* = equilibrium mole fraction active, lb.-moles/lb.-moles total
y_1 = gas inlet mole fraction active, lb.-moles active/lb.-moles total
y_2 = gas outlet mole fraction active, lb.-moles active/lb.-moles total
Δy_{lm} = log mean average mole fraction active, lb.-moles active/lb.-moles total
Y_1 = gas inlet mole ratio active, lb.-moles active/lb.-moles inert
Y_2 = gas outlet mole ratio active, lb.-moles active/lb.-moles inert
Y_t = gas-phase mole ratio active at top of differential section, lb.-moles active/lb.-moles inert
Y_b = gas-phase mole ratio active at bottom differential section, lb.-moles active/lb.-moles inert
z = distance from bottom of bed, ft.
Z = packed height of column, ft.

Greek Letters

α = liquid distribution parameter
ϵ = fraction of packing volume that is gas (void space), cu.ft. gas/cu.ft. packing
ρ_g = gas density, lb./cu.ft.
ρ_l = liquid density, lb./cu.ft.
μ_g = gas viscosity, lb./(hr.)(ft.)
μ_l = liquid viscosity, lb./(hr.)(ft.)

LITERATURE CITED

1. Benoit, R. L., *J. Chem. Eng. Data*, **6**(2), 161 (1961).
2. Chilton, T. H., H. R. Duffey and H. C. Vernon, *Ind. Eng. Chem.*, **29**(3), 298 (1937).
3. Dwyer, O. E., and B. F. Dodge, *ibid.*, **33**(4), 485 (1941).
4. Emerson, M. T., E. Grunwald and R. A. Kromhout, *J. Chem. Phys.*, **33**(2), 547 (1960).
5. Fellinger, L., Sc.D. thesis, Massachusetts Inst. Technol., Cambridge (1941).
6. Kowalke, O. L., O. A. Hougen and K. M. Watson, *Bull. Univ. Wisconsin Eng. Expt. Sta. Ser. No. 68* (1925); *Chem. Met. Eng.*, **32**(10), 443 (1925).
7. Saal, R. N. J., *Rec. Trav. Chim.*, **47**, 73 (1928).
8. Secor, R. M., D.Eng. thesis, Yale Univ., New Haven, Conn. (1958).
9. ———, and R. W. Southworth, *AIChE J.*, **9**(4), 561 (1963).
10. Sherwood, T. K., *Ind. Eng. Chem.*, **33**(4), 424 (1941).
11. ———, and F. A. L. Holloway, *Trans. Am. Inst. Chem. Eng.*, **36**, 21 (1940).
12. Shulman, H. L., and J. E. Margolis, *AIChE J.*, **3**(2), 157 (1957).
13. Shulman, H. L., and W. G. Mellish, *ibid.*, **13**(6), 1137 (1967).
14. Shulman, H. L., C. G. Savini and R. V. Edwin, *ibid.*, **6**(3), 469 (1960).
15. Shulman, H. L., C. F. Ullrich, A. Z. Proulx, and J. O. Zimmerman, *ibid.*, **1**(2), 253 (1955).
16. Shulman, H. L., C. F. Ullrich and N. Wells, *ibid.*, **1**(2), 247 (1955).
17. Vivian, J. E., and T. Schoenberg, *ibid.*, **14**(6), 986 (1968).

Manuscript received May 19, 1969; revision received April 27, 1970; paper accepted April 29, 1970.